IOSR Journal of Applied Chemistry (IOSR-JAC)
e-ISSN: 2278-5736.Volume 18, Issue 8 Ser. I (August. 2025), PP 33-43
www.iosrjournals.org

Synthesis, Characterization And DNA Binding Studies Of Mixed-Ligand Chromium (III) Complexes Of The 2,6 Bis (Benzimidazol-2-Yl) Pyridine

B. Anupama, Sunitha Munagala, Ameena Husain,
D. Shivaleela, E. Udayasree, K. Sharada
Department Of Chemistry, RBVRR Women's College, Hyderabad, Telangana, India.
Govt Polytechnic, Nalgonda, Telangana, India.
Department Of Chemistry, VCIWU, Hyderabad, Telangana, India.
Telangana Tribal Welfare Residential Degree College For Women, Suryapet, Telangana, India
Govt. Polytechnic, Wanaparthy

Abstract
Chromium compounds of the type $[Cr(Bzimpy)(OPD)Cl](Cl)_2$ (1) and $[Cr(Bzimpy)(bipy)Cl](Cl)_2$ (2) (where OPD = orthophenylene diamine, bipy = bipyridine, and Bzimpy = 2,6 bis (benzimidazol-2-yl) pyridine) have been synthesized and studied by analytical and spectroscopic methods such as IR, UV-vis, Mass etc. The complexes' binding behavior to calf thymus DNA (CT-DNA) was studied using spectroscopic methods such as absorption, fluorescence spectra, and viscosity methods. The findings show that the complexes bind to DNA through intercalation. The complex 2 ($1.36\times10^4\ M^{-1}$) has higher binding capacity to CT-DNA than complex 1 ($1.32\times10^4\ M^{-1}$). DNA Cleavage was studied by Agarose gel method.

Keywords: *Chromium complexes, Benzimidazole, DNA binding, DNA Cleavage*

Date of Submission: 03-08-2025 Date of Acceptance: 13-08-2025

I. Introduction

The benzimidazole heterocycle is isostructural with biological nucleotides. This has led to the preparation of its novel derivatives that can be explored in medicinal chemistry. It exhibits a wide range of biological activities like antimicrobial [1], antihypertensives [2] anti-inflammatory [3], analgesic [3], antiparasitic [4], anticonvulsants [5], antitumor [6], antineoplastic [6,7] and cytotoxic activities. This heterocycle also forms a structural component of many chemotherapeutics such as Albendazole, Bendamustine, Omeprazole, Pimobendane, Benomyl, Carbendazim, Telmisartan, Pantoprazole, Etonitazene and Thiabendazole. Moreover, benzimidazole optical sensors have been utilized for bioimaging and in photovoltaics. The structurally diverse lanthanide metal complexes of benzimidazole have exhibited luminescent properties [8, 9].

Chromium metal displays multiple stable oxidation states. It is a biologically essential element involved in biocatalysis and lipid metabolism. Kayser et al. have reported the serendipitous discovery of a benzimidazole-diamide pincer ligand having active methylene group and prepared its chromium complexes [10]. Synthesis, characterization of stable benzimidazole-chromium complexes [11] and their applications like fluorescent properties [1], antimicrobial activities [1], catalysts for polymerization [12], have been reported.

Positively charged complexes, such as those mentioned in current research, are attracted to negatively charged biomolecules like the DNA double helix. The binding of Cr complexes to phosphate group of ATPS has been studied by Kortenkamp et al., using P^{31} NMR spectroscopy [13]. N, N-donors chelating with Cr have reportedly displayed strong binding interactions with DNA [14, 15], also causing plasmid cleavage and protein breakage [16, 17]. Non covalent binding interactions between complexes and the double helix can help reconnoiter cadence of protein synthesis as well as replication process. An awareness of such interactions empowers efficient drug designing and development. It also helps in understanding the type of interaction taking place between them. Shekhar et al have reported groove binding of octahedral water-soluble Cr complexes to CT-DNA [18].

In this work stable octahedral chromium complexes have been prepared and characterized. These complexes exhibit intercalative DNA binding and interaction with the negatively charged phosphate group, which is in agreement with the above-mentioned literatures.

II. Experimental

Materials and Instrumentation

2, 6 pyridine dicarboxylic acid, *o*-phenylene diamine, 1, 10 phenanthroline, Calf Thymus DNA(Genei), Tris HCl buffer, ethidium bromide (EB). The DNA solution in the buffer gave a UV absorbance ratio A_{260}/A_{280} of a about 1.8/1.9 indicating that the DNA was sufficiently free from protein [19] and the concentration of DNA was determined using an extinction coefficient of 6600 $M^{-1}cm^{-1}$ at 260 nm [20]. The stock solution was stored at 4^0C and used after not more than 4 days.

Synthesis of [2, 6-bis (benzimidazole-2yl) pyridine]:

Pyridine -2, 6- di carboxylic acid (3.35g, 20 mM) and *o*-phenylene diamine (4.70g, 44 mM) were mixed with each 20ml of poly phosphoric acid separately. These two solutions were mixed together and heated at 240 ^{0}C on temperature controlled hot plate for 4 hours. The colored solution was poured into 1 liter of vigorously stirred cold water. A blue green precipitate formed was collected by filtration. It is stirred in hot 10% Na_2CO_3 solution (800 ml) for one hour. The resulting solution was filtered and recrystallized from ethanol (Scheme 1) [21].

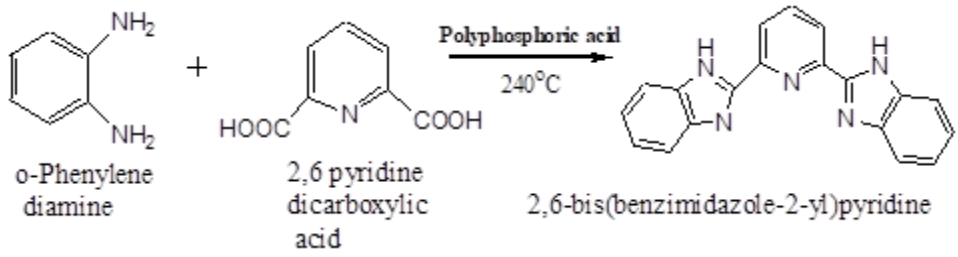

Scheme 1: Reaction scheme for the synthesis of ligand (L)

Data for **[2, 6-bis (benzimidazole-2yl) pyridine]**: FT-IR (cm^{-1}): ν_{NH} 3182, $\nu_{C=N}$ 1573, $\nu_{C=C}$ 1459, $C_{11}H_{13}N_2.2/3H_2O$: Cald.(%); C,70.6; H,4.05; N,21.7. Found (%): C,71.04; H,4.09; N, 21.8, m/Z: 312 (M^++1). H^1-NMR (DMSO-d_6, ppm): 7.3 - 8.3 (aromatic protons),13.3 (Imino proton)[22]

***Synthesis of complexes* 1&2**: To a freshly prepared methanolic solution of $CrCl_3.3H_2O$ (0.2664g,1 mmol), methanolic solution of BZIMPY (0.312g,1 mmol) was added and refluxed at 60^0C for 3 hours. To this solution a methanolic solution of OPDA (0.108g,1 mmol) was added to prepare complex 1 and methanolic solution of Bipy (0.156g, 1 mmol) to prepare complex 2 and refluxed for 5 hours. The product was washed with acetone and evaporated in vacuo over $CaCl_2$.

Data for **$[Cr(Bzimpy)(OPD)Cl](Cl)_2$ (1)**: Dark Green colour

IR(KBr) (cm^{-1}): νN-H 3351, $\nu_{C=N}$ 1571, $\nu_{C=N\ imd}$ 1997, ν_{M-N} 426, Anal. Calc. for $CrC_{25}H_{21}N_7Cl_3$ Cal (%): C (51.90), H (3.63), N (16.95); found (%): C (51.35), H (3.63), N (17.07), µeff: 3.84 BM, UV-vis(nm): 297, 402, 527, 917.

ESI-MS (m/Z);508 **$[Cr(Bzimpy)(OPD)Cl]+ 2H^+$**

Data for **$[Cr\ (Bzimpy)(bipy)Cl](Cl)_2$ (2)**: Brown colour

IR(KBr) (cm^{-1}): νN-H 3342, $\nu_{C=N}$ 1571, $\nu_{C=N phen}$ 1470, $\nu_{C=N\ Imd}$ 998, ν_{M-N} 457; Anal. Calc. for $CrC_{29}H_{21}N_7Cl_3$ Cal (%): C (55.59), H (3.35), N (15.65); found (%): C 55.8, H 3.16, N 15.80, µeff: 3.82 BM, UV-vis(nm):282, 402, 541, 822, 912.

ESI-MS (m/Z); 552 **$[Cr\ (Bzimpy)(bipy)Cl](Cl)_2$**

III. Physical Measurements

The percentage compositions of C, H, and N of complexes and ligand L were determined using micro analytical methods on Perkin Elmer 240C (USA) elemental analyzer. FT-IR spectra of the ligand and its complexes were recorded by using KBr pellets in the range 4000-400 cm^{-1} using Bruker FT-IR spectrometer.

The UV-Visible spectra of the ligand and its metal complexes were carried out in DMSO using Elico SL159 spectrophotometer. ^{1}H NMR spectrum of the ligand was recorded at 200MHz and 300MHz on Varian Gemini Unity Spectrometer using TMS as internal standard. The mass spectra of the compounds were recorded by ESI technique on VG AUTOSPEC mass spectrometer. Magnetic measurements were carried out on a Gouy balance model 7550 using $Hg[Co(SCN)_4]$ as standard. Diamagnetic corrections were carried out by Pascal's constant.

The conductivity measurements were carried out in DMSO (10^{-3}M) using Digisun Electronic Digital conductivity meter.Melting points of the ligand and decomposition temperature of complexes were determined on Polmon instrument (model No.MP-96).

Emission spectra were recorded on a Hitachi RF-2500 Spectro fluorimeter at room temperature.

Thermal melting temperatures were recorded using Hitachi U-2800 double beam UV-Vis spectrophotometer.

IV. Molecular Modeling Studies

Molecular modeling for the proposed structures of metal complexes were carried out by using MM2CS Chem Office version 11.0 molecular modeling program

V. Dna Binding Studies

Electronic absorption titration:

The electronic spectra of complexes 1&2 were monitored in presence and absence of DNA. The binding constant for the interaction of complexes with DNA was obtained from absorption titration data. A fixed concentration of the complexes 1&2 (10 µM) was titrated with increasing amounts of DNA over a range of 10 µM to 100 µM. The binding constant was determined using the following equation,

$[DNA](\varepsilon_A - \varepsilon_F) = [DNA]/ (\varepsilon_B - \varepsilon_F) + 1/ K_b(\varepsilon_B - \varepsilon_F)$ ……..(1)

Where ε_A, ε_F and ε_B correspond to A obsd/[Co], the extinction coefficient for the free metal complex and the extinction coefficient for the metal complex in the fully bound form, respectively. A plot of $[DNA]/(\varepsilon_A - \varepsilon_F)$ Vs. [DNA], gives K_b as the ratio of the slope to the intercept.

Fluorescence titration

Fluorescence spectral studies were performed on Shimadzu Spectrofluorimeter (RF 5301 PC). The fluorescence studies were performed in Tris –HCl buffer at P^H 7.1. Ethidium bromide and DNA solutions was treated with increasing amounts of complexes 1 and 2, in the range of 10-100µM. The fluorescence emission spectra, which corresponds to 600nm were recorded at excitation wavelength 540nm. The DNA and ethidium bromide concentrations were fixed at 10µM and 30 µM respectively. The Stern-Volmer constant K_{sv} calculated by using the following equation.

$I_0/ I = 1+K_{sv}r$

Where I_0 is fluorescence intensity of DNA with complex and I is fluorescence intensity of DNA without the complex. r is the concentration of the complex.

Viscosity measurements:

Viscosity measurements were carried out using an Ostwald viscometer maintained at a constant temperature at 28.0 ± 0.1^0C in a thermostatic bath. Flow time was measured with a digital stopwatch and each sample was measured five times and an average flow time was calculated. Data were presented as $(n/n^o)^{1/3}$versus binding ratio. Where *n* is the viscosity of DNA in the presence of complex and n^o is the viscosity of DNA alone. Viscosity values were calculated from the observed flow time of DNA containing solution corrected for the flow time of buffer alone (t_o) n=t- t_o [23].

VI. Results And Discussion

IR Spectra

In the IR spectra, the distinctive bands at 3182 cm^{-1} and 1490 cm^{-1}, which are attributable to v(NH) stretching and bending vibrations of the ligand [24], are not found in the complexes, showing that complex formation occurs through the -NH group of the imidazole ring. The nitrogen atom of the imidazole ring was confirmed to be coordinated with the metal atom when the imidazole-related peak, which was initially observed at 950 cm^{-1}, shifted to 955–1058 cm^{-1}. The peak in the range of 1492–1573 cm^{-1} is attributed to the v(C=C) and v(C=N) stretching frequencies of Bzimpy, which are shifted to higher frequencies, 1521 cm^{-1} and 1602 cm^{-1} for complex 1. In relation to Bipy, the ring-stretching frequencies of v(C=C) and v(C=N) at 1557 and 1452 cm^{-1} were shifted to 1541 and 1446 cm^{-1}, indicating the coordination of the N atom to Cr(III) ions. The peak v(N-H) of Bzimpy shifted to higher frequencies to 3351 cm^{-1}, in complex 1 & 3342 cm^{-1} in complex 2 indicates, ligand coordinated with metal ion through N-H group. Complexes 1 and 2, far-infrared spectra shows an absorption peak at 250–400 cm^{-1}, which suggests that chloride is present in the coordination sphere (fig 1-2) (Table 1) [25].

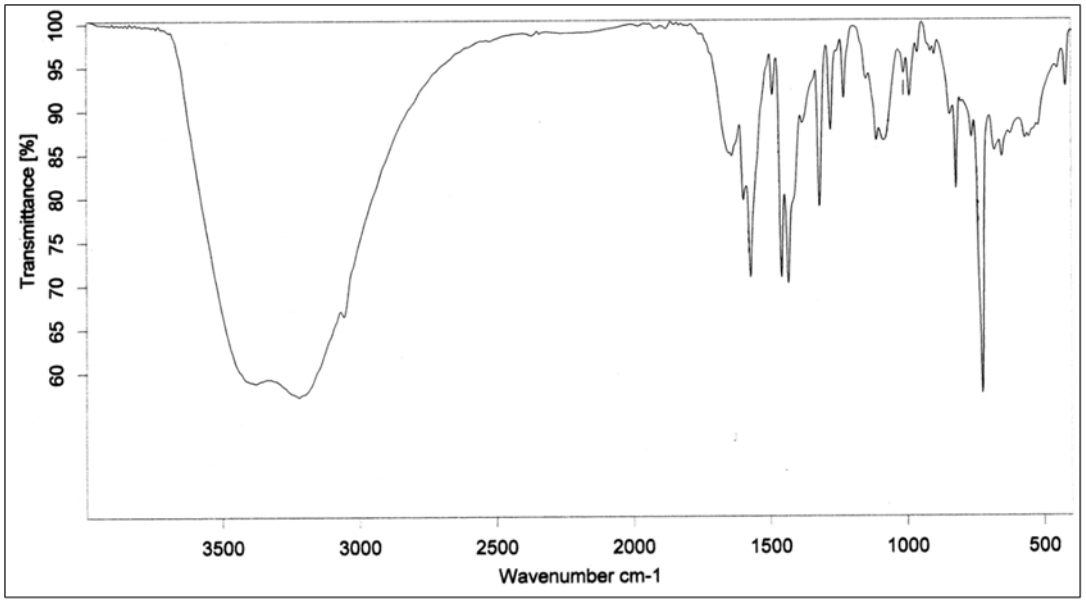

Fig 1. FT- IR spectrum of ligand Bzimpy

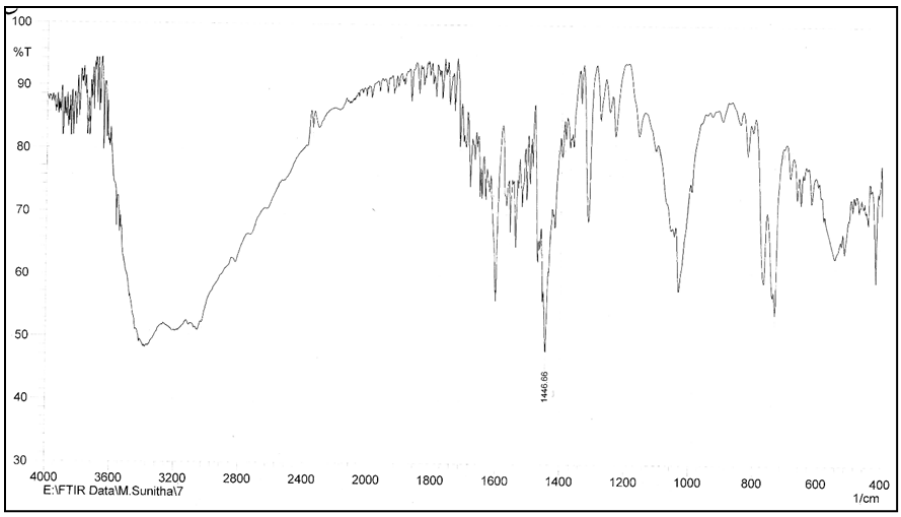

Fig 2. IR spectrum of [Cr (Bzimpy)(bipy)(Cl)]Cl_2

Table 1. FT- IR spectral data of ligand (Bzimpy) and complexes

Compound	V_{NH}	V_{C-H}	$V_{C=N(imd)}$	$V_{C=N(py)}$	$V_{C=C(imd)}$	V_{M-N}	V_{M-Cl}
Bzimpy	3225– 3384	3060	1573	1320	1435	---	---
$[Cr(Bzimpy)(OPD)Cl](Cl)_2$	3351	3061	1571	1321	1452	447	260
$[Cr(Bzimpy)(bipy)Cl](Cl)_2$	3342	3060	1571	1317	1453	463	265

UV-vis Spectra

The d-d transition at 527 nm and 642 nm in the UV-Vis spectra of complexes 1 and 2 respectively (Fig.3), indicating octahedral structure. The bands at 402 nm corresponds to MLCT transitions of complexes 1 and 2. The bands at 222 nm for complex 1 and 282 nm for 2 in UV-Vis spectra were identified as the π-π* transitions of the coordinated OPD or Bipy ligands (Table2).

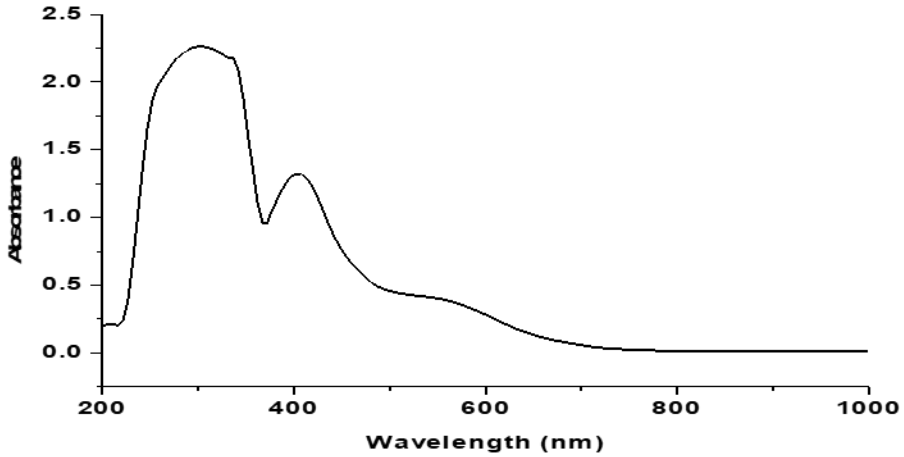

Fig 3. Absorption spectrum of [Cr (Bzimpy)(bipy) Cl] Cl_2

Table 2. UV- VIS spectral data of ligand (Bzimpy) and complexes

Complexes	$\pi - \pi^*$	CT-band	d-d band	Geometry
Bzimpy	222,307	-----	-----	---
[Cr(Bzimpy)(OPD)(Cl)] Cl_2	222	402	527,912	Oh
[Cr(Bzimpy)(bipy)(Cl)]Cl_2	282	402	542,822,912	Oh

At room temperature, the magnetic moments (μeff) of the two complexes (1-2) were 3.84 BM and 3.86 BM, respectively, indicating that they were monomeric complexes. The molar conductance values in DMSO show that the complexes (1,2) are 1: 2 electrolytes

TGA/DTA:

Water molecules in complexes are generally of two types –lattice water and coordinated water [26]. The lattice water will be lost at low temperature (60 -120^{0}C), whereas the coordinated water is lost at higher temperature (150 – 250^{0}C). Thermo gravimetric analysis (TGA) and differential thermal analysis (DTA) of complexes 1 & 2 were carried out at temperature ranges from 0-600^{0}C. In the TGA, DTA of complexes 1 & 2 there was no weight loss in the ranges of temperature 100 – 480^{0}C indicating that absence of coordinated water (Fig.4)

The decomposition of organic part of Cr(III) complexes are on the range 200-470^{0}C, the percent of weight loss is 36.6-38.2.

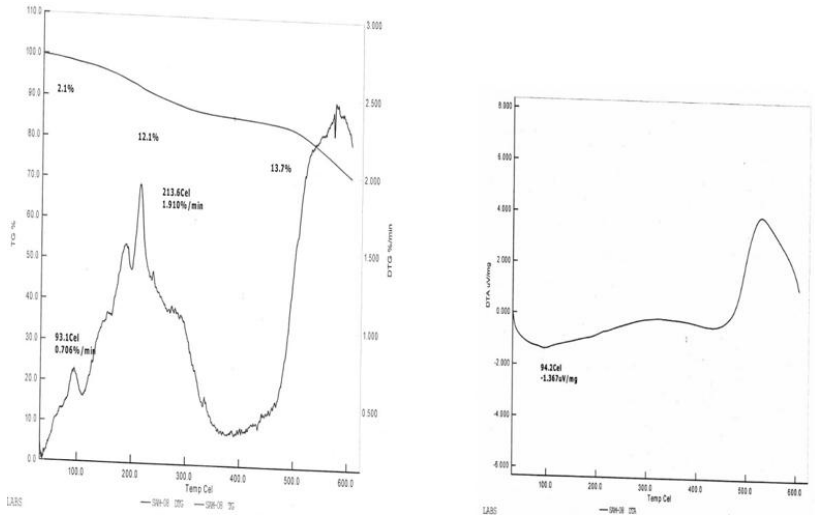

Fig 4. TGA and DTA curves of [Cr(Bzimpy)(bipy)Cl]Cl_2

Mass Spectra

The ESI mass spectra of the complexes 1 [Cr(Bzimpy)(OPD)Cl] Cl_2 and 2 [Cr(Bzimpy)(bipy)Cl] Cl_2 (Fig. 5) molecular ion peaks observed at m/Z 508, 554 respectively, indicating the complexes are in mono positive ions.

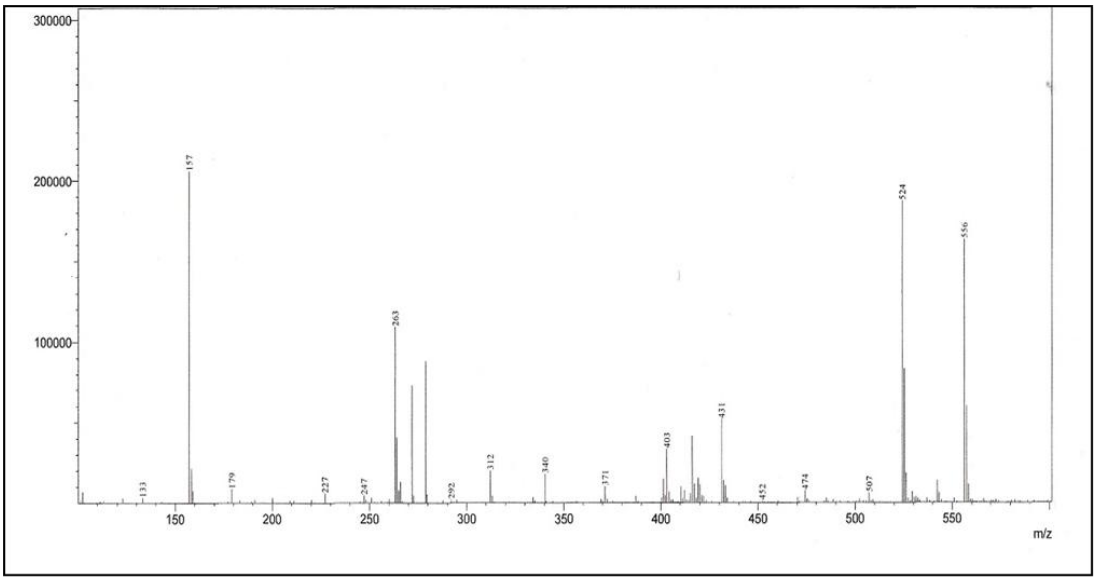

Fig 5. ESI-Mass spectrum of [Cr(Bzimpy)(bipy)Cl](Cl)$_2$

NMR spectra

NMR spectrum (Fig.6) of the ligand (L) and complexes 1and 2 are recorded in DMSO-d6 correspondingly, in order to clarify the structural characteristics of the compounds. The ligand's NMR spectra show a band at about 13.3 ppm that is caused by the -NH protons. Phenyl protons were allocated to 7.3–8.3 ppm [27]. The absence of a -NH proton signal at 13 ppm indicates coordination with metal.

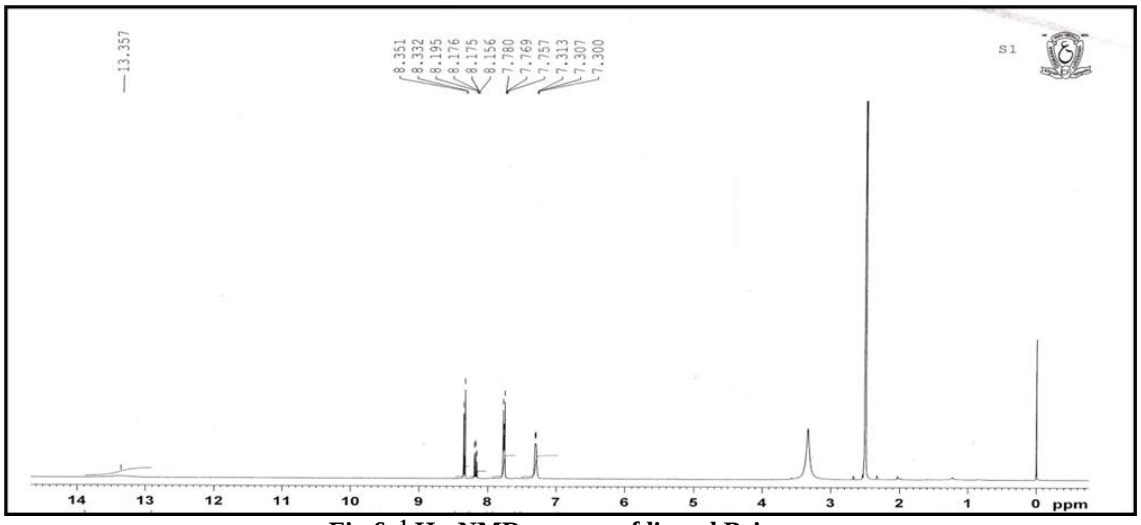

Fig 6. ^{1} H - NMR spectra of ligand Bzimpy

Molecular modelling Structures

In the absence of crystal data, it was thought worthwhile to obtain structural information through molecular modeling. The ball and stick representation of complexes 1&2 (Fig.7) obtained through molecular modeling calculations using MM2CS Chem Office version 11.0 are represented below

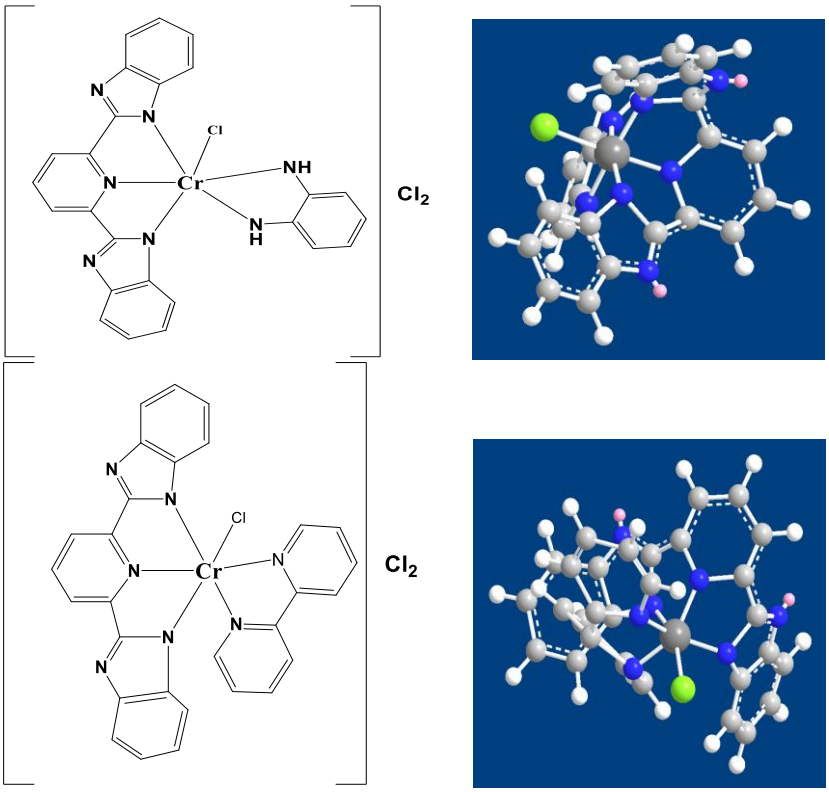

Fig 7. Energy minimized structures of complexes [Cr (Bzimpy)(OPD)Cl]Cl_2 (1) and [Cr (Bzimpy)(bipy)Cl]Cl_2 (2)

DNA binding

Electronic absorption titration:

Absorption spectra were used to study the complexes' interactions with DNA [24]. Absorption Spectra of complexes (1 and 2) at constant complex concentration with and without CT-DNA are shown in (Figs. 8). MLCT transition bands of complexes 1 and 2 showed bathochromism and hypochromism, respectively, as the concentration of DNA increased. These spectral features indicate that the complexes and DNA are interacting with each other.

The intrinsic binding constants (K_b) of complexes containing calf thymus DNA were calculated from the decay of the absorbance monitored for complexes in order to objectively compare the binding strengths of the two complexes. Equation 1 was used to calculate the intrinsic binding constant K_b of the complexes containing CT-DNA [28].

The absorbance decay yielded the intrinsic binding constant (K_b) for complexes 1 and 2, which were around 1.32×10^4 M^{-1} and 1.36×10^4 M^{-1}, respectively. The larger planar area of the bipy ligand in complex 2 may be responsible for its superior DNA binding capabilities over complex 1.

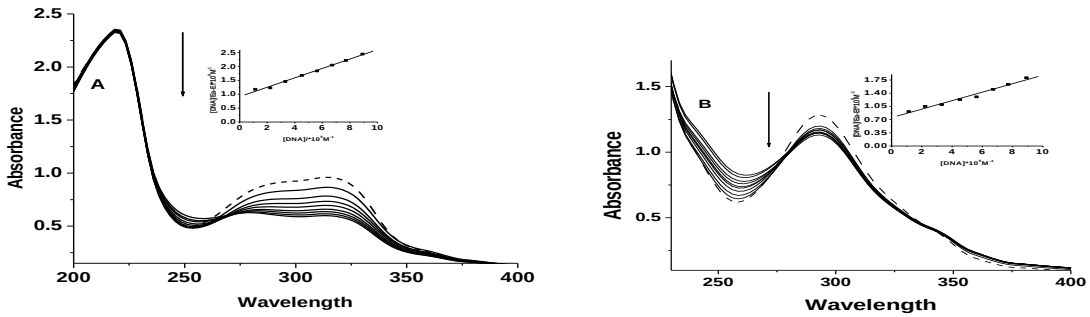

Fig 8 Absorption spectra of complex 1[Cr (Bzimpy)(OPD)Cl] Cl_2 (A), and complex 2 [Cr (Bzimpy)(bipy)Cl]Cl_2 (B) in the absence (---) and presence (—) of increasing amounts of DNA. [DNA] = 10 – 100 µM. ([DNA] =1.727×10^{-4}M). Arrow shows the absorbance changes upon increasing DNA concentration. Inset: Linear plots for the calculation of intrinsic binding constant K_b.

Competitive binding:

When DNA is present, Ethidium Bromide (EB) produces a bright fluorescence light because of the significant intercalation between the neighboring DNA base pairs. A second molecule can be added to extinguish the increased fluorescence, according to earlier reports [29,30]. The degree of binding between the second molecule and DNA is ascertained by measuring the quenching extent of fluorescence of EB attached to DNA.

The emission spectra of EB bound to DNA are shown with and without Cr(III) complexes (Fig.9). When complexes 1 and 2 are added to DNA that has been pretreated with EB, there is a noticeable decrease in emission intensity, suggesting that the complexes compete with EB for DNA binding.

According to the classical Stern – Volmer equation [30]:

$I_o/ I = 1+K_{sv}r$

K_{sv} is a linear Stern-Volmer quenching constant that depends on the ratio of the bound concentration of EB to the concentration of DNA, where r is the ratio of the total concentration of complex to that of DNA, and I_0 and I are the fluorescence intensities in the absence and presence of complex, respectively.

Figure 9 displays the fluorescence quenching curves of EB attached to DNA by 1 and 2. The quenching plots demonstrate that the linear Stern-Volmer equation, which verifies that two complexes bind to DNA, and the quenching of EB bound to DNA by complexes 1 and 2 are in good accord. K_{sv} in the Io/I Versus [complex]/[DNA] linear fit plot is determined by the slope to intercept ratio. K values for 1 and 2 are, respectively, 0.193 and 0.205 (Table 3).

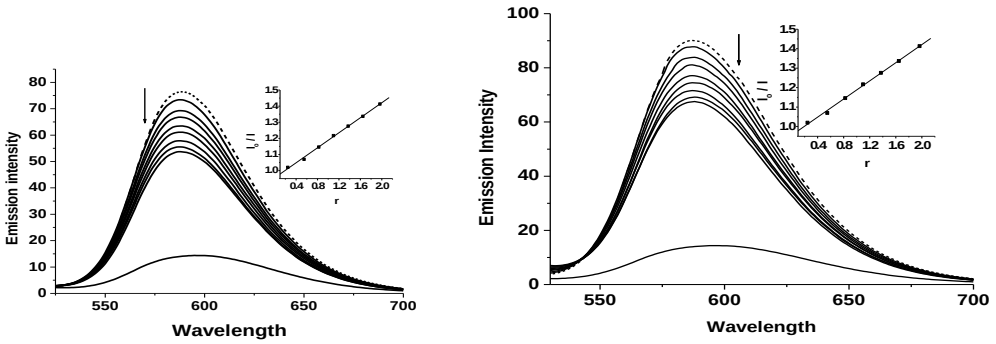

(A) (B)

Fig.9.Emission spectra of EB bound to DNA ([DNA] =2.33×10^{-5}M) in the absence (----) and presence (—) of complexes (10 µM) [Cr (Bzimpy)(OPD)Cl]Cl_2 (A) and [Cr(Bzimpy)(bipy)Cl]Cl_2 (B), Inset: Stern-Volmer quenching curves.

Table 3. DNA binding affinities of complexes 1 & 2

Complex	K_b	K_{sv}
[Cr(Bzimpy)(OPD)(Cl)]Cl_2	1.32×10^4	0.193
[Cr(Bzimpy)(bipy)(Cl)]Cl_2	1.36×10^4	0.205

Viscosity measurements:

Viscosity measurements were done, for additional support of the binding of complexes with DNA. Viscosity of DNA increased by intercalative interaction of complexes. Due to elongation of DNA helix as base pairs are cleaved to bind with complex. The viscosity of the DNA also enhanced by Ethidium bromide intercalator. In our experiment, the increased amounts of complexes were added to DNA (at constant concentration), which enhances the viscosity of DNA (Fig.10) same as EB. This resulting data suggesting that the complexes bind to DNA by intercalative mode [31,32].

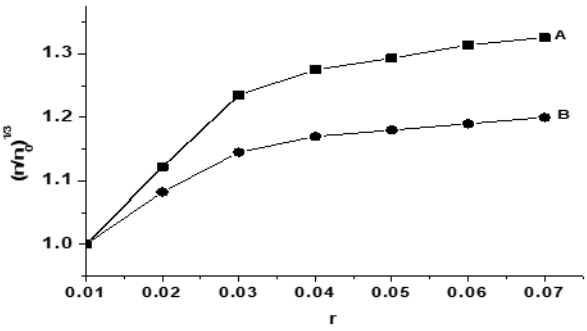

Fig. 10. Effects of increasing amount of complexes [Cr (Bzimpy)(OPD)Cl]Cl_2 (B) and [Cr (Bzimpy)(bipy)Cl]Cl_2 (A) on the relative viscosity of CT-DNA at 29ºC ± 0.1, [DNA] = 15 µM

Thermal Denaturation:

Experiments were conducted for thermal denaturation of DNA in the absence and presence of complexes 1 & 2 **[Cr(Bzimpy)(OPD)Cl](Cl)$_2$** and **[Cr(Bzimpy)(bipy)](Cl)$_3$** for obtaining melting temperatures (T_m) Profiles. Interaction of small molecules with double helical DNA is known to increase or decrease the melting temperature (T_m), the temperature at which the double helix denatures into single standard DNA [33]. It is well known that an increase in T_m means an intercalative or phosphate binding whereas decrease is indicating of base binding. The melting temperatures were determined by monitoring the absorbance of the DNA at 260 nm as a function of temperature. The T_m of CT-DNA was observed at 75 $\pm$ 1^0C. The T_m of DNA in the presence of complexes are shown in figs 11 & 12 increased by 5 - 9^0C. These results provide evidence for intercalative; phosphate binding of the complexes does leads to an increase in ΔT_m of DNA.

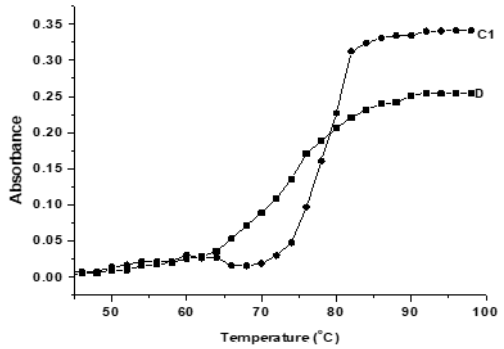

Fig 11. Thermal denaturation profile of CT - DNA (1.727×10^{-4}M)) in aqueous buffer before (curve D) and after (curve C1) addition of [Cr(Bzimpy)(OPD) Cl](Cl)$_2$ (1.727×10^{-4}M).

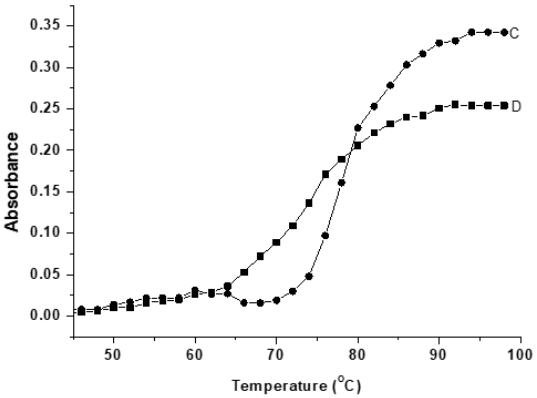

Fig 12. Thermal denaturation profile of CT - DNA (1.727×10^{-4}M)) in aqueous buffer before (curve D) and after (curve C) addition of [Cr(Bzimpy)(Bipy) Cl](Cl)$_2$ (1.727×10^{-4}M).

DNA Cleavage Studies:

Gel electrophoresis experiments using pUC19 DNA were performed with complexes in the presence and absence of H_2O_2 as an oxidant. The nuclease activity was greatly enhanced by the incorporation of metal ion in the respective copolymer; it is evident from Fig. 13, which shows that the complexes 1 and 2 cleave DNA more efficiently in the presence of oxidant, which may be due to the formation of hydroxyl free radicals. The production of hydroxyl free radical is due to the reaction between the metal complex and oxidant. These hydroxyl radicals participate in the oxidation of the deoxyribose moiety, followed by hydrolytic cleavage of the sugar phosphate backbone (34). The more pronounced nuclease activity in the metal complexes in the presence of oxidant may be due to the increased production of hydroxyl radicals. The cleavage efficiency was measured by determining the ability of the complex to convert the super coiled DNA to nicked (open circular) form or sheared form. As it is evident from Fig. 13, there is a considerable increase in the intensity of bands for open circular form in the case of complexes 1 & 2. This suggests that samples have nicking activity.

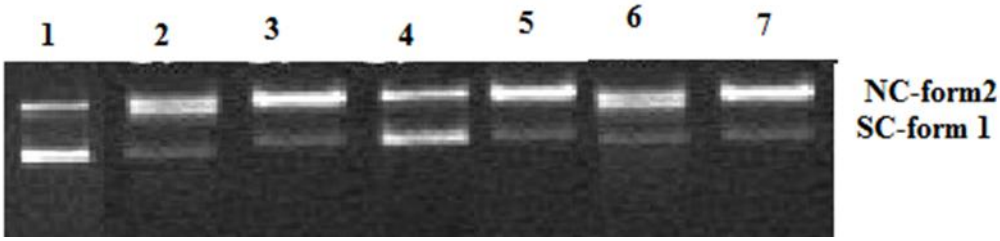

Fig 13. Changes in the Agarose gel electrophoresis pattern of pUC18 plasmid DNA, induced by H_2O_2 and metal complexes: DNA alone (1); DNA +[Cr (Bzimpy)(OPD) Cl]Cl_2 + H_2O_2 (6); DNA+ [Cr (Bzimpy)(bipy)Cl)]Cl_2 + H_2O_2 (6)

VII. Conclusion

In summary the two novel octahedral Cr (III) complexes 1 & 2 with the ligand 2,6 bis(benzimidazol-2-yl)pyridine were synthesized, characterized and their DNA binding and cleavage properties were investigated. The complexes bind to CT-DNA through intercalation and binding to phosphate group of DNA. The binding constants of complexes 1 and 2 to CT-DNA have been determined by absorption titrations and spectrofluorimetric method. The complex 2 shows higher binding capacity to CT-DNA than complex 1 due to its planarity and greater surface area.

Conflict Of Interest

The authors declare that there is no conflict of interests regarding the publication of this article.

References

[1] S. Rastegarina, M. Pordel, S. Allameh, Arabian Journal Of Chemistry. 2020, 13(2),3903-3909
[2] Y.Zhang, J.Xu, Y. Li, H. Yao, X. Wu, Chemical Biology And Drug Design,. 2015, 85,(5), 541-548
[3] M. Gaba, S. Singh, C. Mohan, European. Journal Of Medicinal. Chemistry, 2014, 9(76)494-505
[4] P. Flores-Carrillo, J. Vela´ Zquez-Lo´ Pez, R. Aguayo-Ortiz, A. Hernandez-Campos, P. Trejo-Soto, L. Yepez-Mulia, R. Castillo, European. Journal Of Medicinal. Chemistry. 2017, 137,211-220
[5] N. Siddiqui, M. S. Alam, R. Ali, M. S. Yar, O. Alam, Medicinal Chemistry Research, 2016, 25,1390-1402
[6] D.H. Romero, S.R. Luna, G.L. Monteon, A. C. Navarro, J. Antonio, P. S. Raul, Coordination Chemistry Reviews. 2021, ,439, 213930
[7] Nguyen Vt, Huynh Tk, Ho Gt, Nguyen Th, Le Anh Nguyen T, Dao Dq, Mai Tvt, Huynh Lk, Hoang Tk. Royal Society Open Science, 2022 , 9, 220659.
[8] A. C. Navarro, D.H. Romero, A. F. Parra, J. M. Rivera, S. E. C. Blum, R. C. Peralta, Coordination Chemistry Reviews,2021, 427,213587
[9] A. C. Navarro, S.R. Luna, J. M. Rivera, M. Rodriguez, A. F. Parra, S. C. Blum, R. C. Peralta, Journal Molecular. Structure, 2023, 1283, 135345
[10] A. K. Kayser, P.T. Wolczanski, T. R. Cundari, S. N. Macmillan, M. M. Bollmeyer, Chemical Communications.2022, 70,
[11] A.V. Grishin, E. V. Sazonova, N. V. Somov Et Al. Russian Journal Of Coordination Chemistry, 2025, 51, 19-29.
[12] W. Luo, A. Li, S. Liu, H. Ye, And Z. Li, Organometallics, 2016,35(17), 3045-3050.
[13] A. Korte Kamp And P. O'brien, Detmar Beyersmann, Carcinogenesis, 1991, 12(6),1143–1144,
[14] H. Y. Shrivastava, B. U. Nair, Biochemical And Biophysical Research Communications,285(4) 27 ,2001, 915-920.
[15] R. Vijayalakshmi, V. Subramanian, B. U. Nair, Journal Of Biomolecular Structure And Dynamics, 2002, 19, 1063-1071.
[16] R. Vijayalakshmi, V. Subramanian, B. U. Nair, , Journal Of Biomolecular Structure And Dynamics, 2002, 19, 1063-1071
[17] L. Joudah, S. Moghaddas, R. N. Bose, Chemistry.Communication. 2002,16, 1742-1743.
[18] B. Shekhar, K. Rajeshwari, B. Jaysree And P. V. A. Lakshmi, Applied Organometallic Chemistry,2022, 36(4),E6601.
[19] J. Marmur, Journal Of Molecular Biology, 1961, 3 (2), 208-218.
[20] M.F.Reichmann,S.A.Rice,C.A.Thomas,P.Doty, Journal Of The American Chemical Society,1954,7(11),3047.
[21] A.W.Addison, P.J.Burke, Journal Of Heterocyclic Chemistry,1981, 18(4), 803-805.
[22] M.Yadama,Y.Tanaka,Y.Yoshimoto,S.Kuroda,I.Shimao, Bulletin Of The Chemical Society Of Japan,1992,65(4), 1006-1011.
[23] M. Eriksson, M. Leijon, C. Hiort, B. Norden, A. Graslund, Biochemistry.1994, 33, 5031 -5040 .

[24] B.Mohani,F.Arjmand,And S.Tabassum, European Journal Of Medicinal Chemistry,2005,40(11), 1103-1110 .
[25] N.Raman,A. Kulandaisamy,K.Jayasubriamanian, J.Indian.Chem,2002,41(A), 942-949.
[26] C.H.Krishna,C.M.Mahapatra,K.C.Dush. Journal Of Inorganic And Nuclear Chemistry,1977,39(7),1253-1258
[27] J.Ruiz,R.Quesada,V.Riera,S.G.Granda,M.R.Diaz,Chemical Communications,2003,16,2028-2029.
[28] J.K.Barton, A.Danishefsky, J.Goldbe, Journal Of The American Chemical Society,1984,106,2172-2176.
[29] A.Wolf, G. H. Shimer Jr, T. Meehan, Biochemistry,1987, 26, 20, 6392–6396.
[30] B.C. Baguley, M.Lebret, Biochemistry,1984,23,937.
[31] J. R. Lakowicz, G. Webber, Biochemistry, 1973, 12, 4161.
[32] S. Sathyanarayana, J.C. Dabrowiak,J.B. Chairs,Biochemistry.1992,31,9319-9324.
[33] S.Sathyanarayana,J.C.Dabrowiak,J.B.Chairs,Biochemistry,1993,32,2573-2584.
[34] T. A. Tysoe, A. D. Baker And T . C. Strekas. The Journal Of Physical Chemistry. 1993, 97, 1707-1711